Turk J Elec Engin, VOL.14, NO.1 2006, © TÜBİTAK

Complex Analysis of the Lossy-Transmission Line Theory: A Generalized Smith Chart

E. GAGO-RIBAS[1], **C. DEHESA-MARTİNEZ**[2], **M. J. GONZÁLEZ-MORALES**[2]
[1]*Area de Teoría de la Señal y Comunicaciones*
Dpto. Ingeniería Eléctrica, Electrónica de Computadores y de Sistemas
Universidad de Oviedo-SPAIN
[2]*Dpto. de Teoría de la Señal y Comunicaciones e I. T.*
Universidad de Valladolid-SPAIN
e-mail: egr@tsc.uniovi.es, cardeh@rest.tel.uva.es, gonmor@yllera.tel.uva.es

Abstract

It has been very usual in the specialized literature to skip the detailed study of the lossy transmission line theory by reducing it to the low-loss approximation. Although this is valid in the most common practical cases, the study of the general lossy case becomes very important due to the fact that it makes possible a better and deeper understanding of the physical effects associated to general losses, as well as the low-loss frequency-dependent regime. Besides, the analysis of the general case provides important results that may be extended to the analysis of real waveguiding systems, facilitating the understanding and description of their physical behavior. The present paper deals with the analysis of the most important parameters involved in the general lossy transmission line theory by introducing a general methodology based on their complex analysis. This methodology let us to understand and predict the physical behavior of a lossy transmission line problem by means of very intuitive graphical representations. As a particular result, the concept of a generalized Smith chart will appear. As a consequence, this general analysis covers the usual lossless and low-loss cases, providing a clear methodology that may be properly used for both educational and professional purposes. This methodology has been also implemented into a suitable software tool which serves as a perfect complement to visualize and understand the underlying analysis, thus improving the educational possibilities of this kind of generalized analyses.

Key Words: *Complex analysis, losses, low-loss approximation, transmission lines, generalized Smith chart.*

1. Introduction

There is a lack in the literature about transmission line and waveguide theories (refer, for instance, to [1]-[3]) in the detailed study of the general lossy transmission line case. This may be probably due to the belief that this theory is not considered important enough since the general assumption in the design of a real transmission line or waveguide system is to minimize the signal loss during propagation. Although this is true, the author considers that the complete understanding of the lossy transmission line theory may become very important from both the educational and the practical points of view.

The importance from the educational side comes from the fact that, usually, the expressions associated to the lossy transmission line theory are much more complicated to analyze that in the ideal case, and also than those in the low-loss approach. Moreover, the last one, defined by the usual conditions $R << \omega L$ and $G << \omega C$, with R, L, G and C denoting the series distributed resistance and inductance, and the shunt distributed conductance and capacitance, all per unit length, typical in the lossy equivalent transmission line circuit, may be understood much more better if performing a complete study of the general lossy regime. All those difficulties may be avoided by using the *complex analysis* presented in this paper which let us to generalize all the results by means of graphical representations that provide us with clear interpretations and descriptions to the solutions of the difficult mathematical expressions involved in the usual analysis.

The practical interest comes from the fact that the well understanding of the lossy theory and the complex analysis methodology may become very useful for the analysis and design of special devices based on the physical effects associated to losses, and also for the possibility to establish equivalent circuits of new electromagnetic problems involving lossy media.

As will be summarized in this paper, the complexity of the expressions appearing in the general analysis of the lossy transmission line theory may be simplified and, thus, better analyzed by performing a detailed discussion of the magnitudes involved in the analysis directly in their own complex domains (assuming time-harmonic dependence $e^{j\omega t}$). It is also convenient to obtain expressions in which the parameters associated to the effects due to the conductors and the dielectrics in a real waveguide system[1] appear in well differentiated terms in order to parameterize better those effects. The obtained results will be easily verified to solve also the lossless (ideal) case when making $R = G = 0$ in the general expressions, and the analyses of the complex characteristic impedance $Z_c = [(R + j\omega L)/(G + j\omega C)]^{1/2}$ and the complex propagation constant $\gamma = \alpha + j\beta = [(R + j\omega L)(G + j\omega C)]^{1/2}$ in terms of frequency will provide a clear description of the general effects associated to losses, leading also to clarify the low-loss approximation regime.

The generalization of previous results together with the analysis of the reflection coefficient $\rho(z) = \rho'(z) + j\rho''(z)$, and the wave impedance $Z(z) = |Z(z)| \exp(j\varphi_Z(z))$ in any arbitrary point of the transmission line, leads to the definition of a generalized Smith chart in the complex ρ-plane, and the corresponding analysis in the complex $Z-$plane, which let us graphically visualize the behavior of a general lossy transmission line parameterized in terms of the phase of the characteristic impedance, namely φ_{Z_c} throughout the paper.

All these results may be appropriately extended into the waveguide theory, making possible a better and more realistic understanding of some of the propagation models appearing in the solution of ideal waveguides, for instance, the ideal concept of an evanescent mode appearing under cutoff frequency regimes interpreted as the limiting case of a real propagating mode with large values of the attenuation constant α and very small values of the phase constant β.

2. General description of the problem

In the present paper, it will be assumed that the reader is familiar with both the lossless transmission line theory and the low-loss approximation. The usual equivalent circuit for a lossy transmission line, Figure 1, defined by the basic parameters R, L, G and C, assuming a time-harmonic representation in the form $\exp(j\omega t)$, leads to the usual complex representation of voltages and currents in an arbitrary point z of the

[1] The present analysis is only valid for real waveguiding systems supporting quasi-TEM modes (under Leontovich approximation). The lossy equivalent circuits for other modal solutions may follow a straight parallel procedure to that described in this paper.

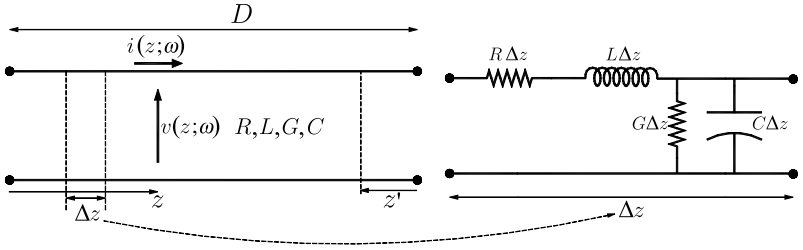

Figure 1. Equivalent differential circuit of a lossy transmission line in terms of the series distributed resistance and inductance, R and L, and the shunt distributed conductance and capacitance, G and C, all per unit length. The position in the line is represented by z or z' according to the chosen origin, generator or load respectively.

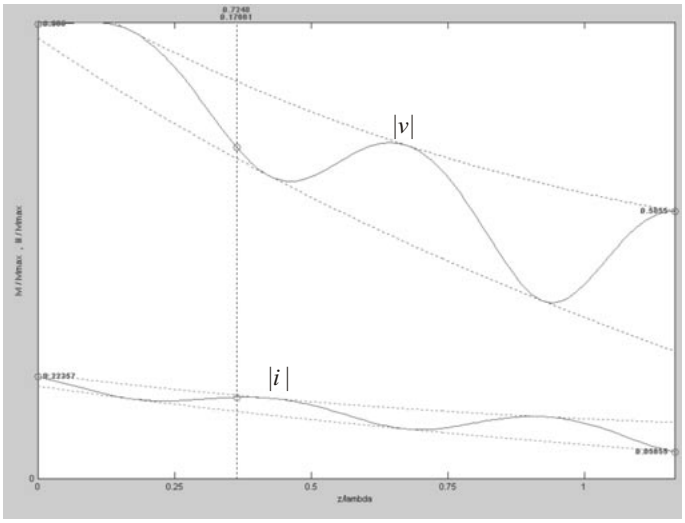

Figure 2. An example of the usual behavior of $|v|$ and $|i|$ along a 0.8 cm lossy transmission line. The results have been obtained at 1.0 GHz with a 10 Ω load resistive impedance, considering the following basic parameters: $L = 0.7$ μH/m, $C = 30$ nF/m, $R = 120$ Ω/m, and $G = 40$ $(\Omega\,\mathrm{m})^{-1}$.

transmission line,

$$v = v^+ + v^- = v_0^+ e^{-\gamma z} + v_0^- e^{+\gamma z}, \tag{1}$$

$$i = i^+ - i^- = \frac{v_0^+}{Z_c} e^{-\gamma z} - \frac{v_0^-}{Z_c} e^{+\gamma z}, \tag{2}$$

$$\rho = \frac{v^-}{v^+} = \frac{i^-}{i^+}, \tag{3}$$

$$Z = \frac{v}{i}, \tag{4}$$

with $v \equiv v(z;\omega)$ and $i \equiv i(z;\omega)$ denoting the z-dependent total voltage and current phasors, $v^+ \equiv v^+(z;\omega)$ and $i^+ \equiv i^+(z;\omega)$ the z-dependent incident voltage and current phasors, $v^- \equiv v^-(z;\omega)$ and $i^- \equiv i^-(z;\omega)$ the z-dependent reflected voltage and current phasors, v_0^+ and i_0^+ the incident voltage and current phasors

at $z = 0$, and v_0^-, i_0^- the reflected voltage and current phasors at $z = 0$. This means that the behavior of voltages and currents along the line (refer to Figure 2 for an example of the typical shapes of $|v(z;\omega_0)|$ and $|i(z;\omega_0)|$ or stationary wave pattern, SWP, along a lossy TL) will be determined and described by the basic parameters (the characteristic impedance, $Z_c \equiv Z_c(\omega)$, and the propagation constant, $\gamma \equiv \gamma(\omega)$) as well as the wave parameters (the wave impedance, $Z \equiv Z(z;\omega)$, and the reflection coefficient, $\rho \equiv \rho(z;\omega)$); their expressions may be summarized as follows:

- The *basic parameters* in terms of R, L, G and C are given by the well-known equations[2],

$$Z_c = \sqrt{\frac{Z_s}{Y_p}}, \tag{5}$$

$$\gamma = \sqrt{Z_s Y_p}, \tag{6}$$

with

$$Z_s = R + j\omega L, \tag{7}$$

$$Y_p = G + j\omega C. \tag{8}$$

Thus, the analysis of the behavior of Z_c and γ presented in Sec. 3 will require an initial study of the complex magnitudes Z_s and Y_p, Sec. 2.1.

- The *wave parameters* in terms of Z_c and γ are given by the well-known equations,

$$\rho = \frac{Z - Z_c}{Z + Z_c}, \tag{9}$$

$$Z = Z_c \frac{1+\rho}{1-\rho}, \tag{10}$$

or

$$\rho = \rho_L e^{-2\gamma z'}, \tag{11}$$

$$Z = Z_c \frac{Z_L \cosh(\gamma z') + Z_c \sinh(\gamma z')}{Z_c \cosh(\gamma z') + Z_L \sinh(\gamma z')}, \tag{12}$$

with ρ and Z in (11)-(12) written in terms of z' (coordinate referred to the load, Figure 1). Although expressions (9) and (10) are formally identical to those in the ideal lossless case, their behavior is quite different due to the different behavior of ρ. Notice that equations (9) and (10) establish a functional relation between two complex quantities that may be analyzed and visualized as complex transformations or mappings between the corresponding complex planes. In particular, this paper will deal with: (i) the description of the behavior of $\rho(Z)$ in the complex Z-plane, eq. (9), for the general lossy case as will be presented in Sec. 4, and (ii) the representation of $Z(\rho)$ in the complex ρ-plane, eq. (10), arising to the concept of the generalized Smith chart which will be introduced in Sec. 5.

[2]This paper is based on the ideal assumption that the parameters R, L, G and C are not frequency dependent.

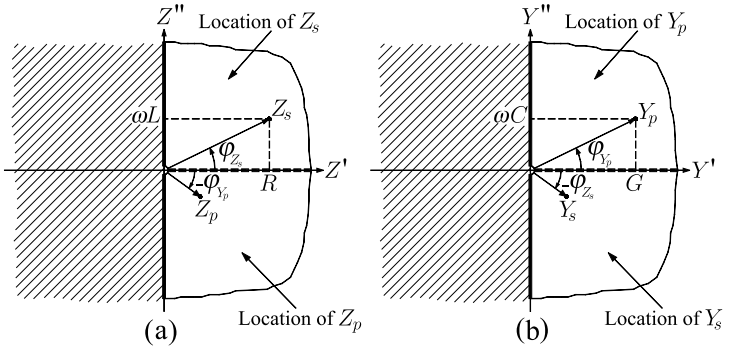

Figure 3. Location of Z_s, Z_p, Y_s and Y_p in the complex Z- and Y-planes.

2.1. Complex characterization of Z_s and Y_p

The series impedance and the shunt admittance defined in (7)-(8) may be analyzed by recalling that $R \geq 0$ and $G \geq 0$. Notice that, for the ideal case, denoted by subscript 0, $c_{e0} = 1/\sqrt{LC}$ represents the phase velocity which may be as much as $c_0 \approx 3 \times 10^8$ m/s for the case of propagation in a vacuum. This means that $LC = 1/c_{e0}^2 \geq 1/c_0^2$, which makes L and C to be always different from zero.

After this initial consideration, it is possible to determine the complex values associated to (7)-(8). The values of $Z_s = |Z_s| \exp(j\varphi_{Z_s})$ will lay on the first quadrant of the Z-complex plane ($Z = Z' + jZ''$) as shown in Figure 3(a), excluding the origin and the real axis,

$$|Z_s| > 0, \qquad \varphi_{Z_s} \in (0, \pi/2]. \tag{13}$$

Similar considerations may be done for Y_p in the Y-complex plane ($Y = Y' + jY''$), Figure 3(b),

$$|Y_p| > 0, \qquad \varphi_{Y_p} \in (0, \pi/2]. \tag{14}$$

The associated values of $Y_s = 1/Z_s$ and $Z_p = 1/Y_p$ are also shown in Figure 3,

$$|Y_s| = \frac{1}{|Z_s|} > 0, \qquad \varphi_{Y_s} = -\varphi_{Z_s} \in [-\pi/2, 0), \tag{15}$$

$$|Z_p| = \frac{1}{|Y_p|} > 0, \qquad \varphi_{Z_p} = -\varphi_{Y_p} \in [-\pi/2, 0). \tag{16}$$

With these basic ideas in mind, we will be able to analyze the behavior of the basic parameters Z_c and γ.

3. Basic parameters in terms of frequency

Let us present in this section the main results corresponding to the complex analysis of the basic parameters Z_c and γ, as well as some related conclusions concerning phase velocities, loss effects, and the low-loss approximation. A more detailed analysis of these parameters may be found in [4].

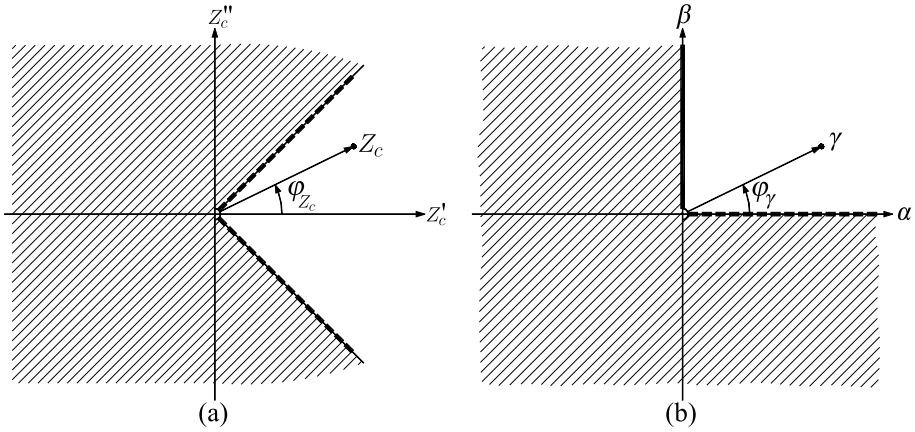

Figure 4. Validity regions of the values of Z_c and γ in their own complex planes.

3.1. Characteristic impedance

The characteristic impedance in (5) may be easily analyzed in terms of the behavior of Z_s and Y_p in (7)-(8). From the complex transformation in (5), it may be shown that $Z_c(\omega) = |Z_c|\exp(j\varphi_{Z_c})$ will satisfy $\varphi_{Z_c} = \varphi_{Z_s}/2 - \varphi_{Y_p}/2$, if we consider the principal value of the square root. This condition becomes in practice,

$$|Z_c| > 0, \qquad \varphi_{Z_c} \in [-\pi/4, \pi/4], \tag{17}$$

relation which defines the limits for the possible values of the characteristic impedance in the Z_c-complex plane as shown in Figure 4(a). The expression of Z_c may be easily written as,

$$|Z_c| = Z_{c0}\left[\frac{1 + R^2/\omega^2L^2}{1 + G^2/\omega^2C^2}\right]^{1/4}, \tag{18}$$

$$\varphi_{Z_c} = \frac{1}{2}\tan^{-1}\left(\frac{\omega L}{R}\right) - \frac{1}{2}\tan^{-1}\left(\frac{\omega C}{G}\right), \tag{19}$$

equations which maintain the well differentiated terms due to both the conductors (R, L) and the dielectrics (G, C) of a real waveguide system. The parameter $Z_{c0} = \sqrt{L/C}$ denotes the characteristic impedance of a lossless transmission line which is a real quantity. Notice that $|Z_c| \to Z_{c0}$ and $\varphi_{Z_c} \to 0$ when $R \to 0$ and $G \to 0$. The behavior of (18) and (19) in terms of ω for different values of R, L, G and C are shown in Figure 5. Notice that all values of φ_{Z_c} satisfy the condition in (17). It is important to remark that the simple methodology summarized in this section provides a good comprehension of the real behavior of Z_c, something that is more difficult to achieve through the directly developed expression of (5) in terms of R, L, G and C.

3.2. Propagation constant

The propagation constant in (6) characterizes the z-dependence of the amplitude of v^+, v^-, i^+ and i^- in (1)-(2) through its real part α, maintaining the description of the propagation characteristics of

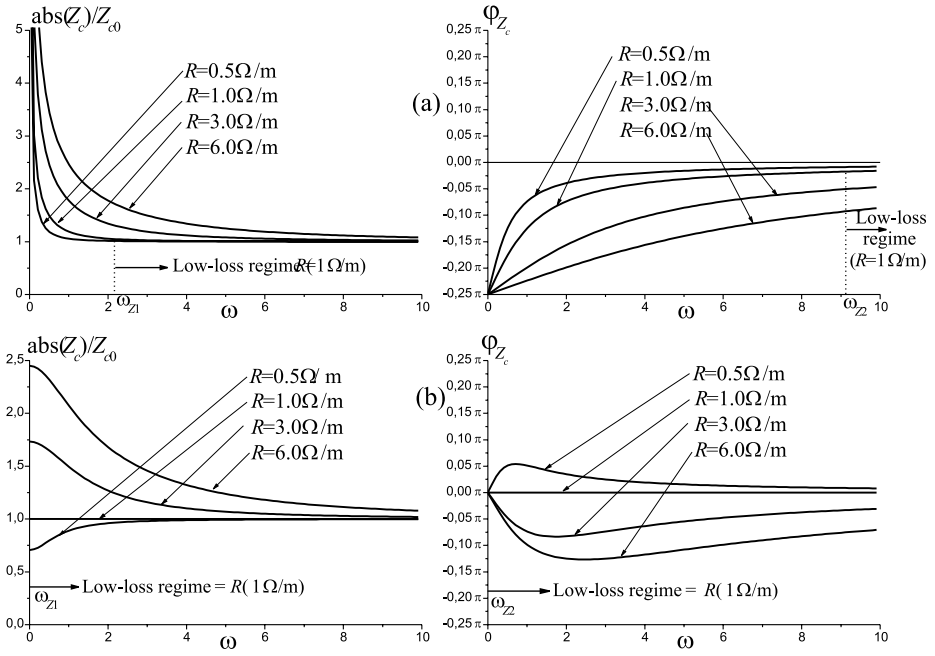

Figure 5. Representation of the characteristic impedance, $|Z_c|$ and φ_{Z_c}, in terms of R when $L = 1$ H/m, and $C = 1$ F/m, for the cases with: (a) $G = 0$ $(\Omega\mathrm{m})^{-1}$, and (b) $G = 1$ $(\Omega\mathrm{m})^{-1}$. The corresponding low-loss regimes (ω_{Z1} and ω_{Z2}), approximated in (a) and exact in (b), are indicated for the case with $R = 1$ Ω/m.

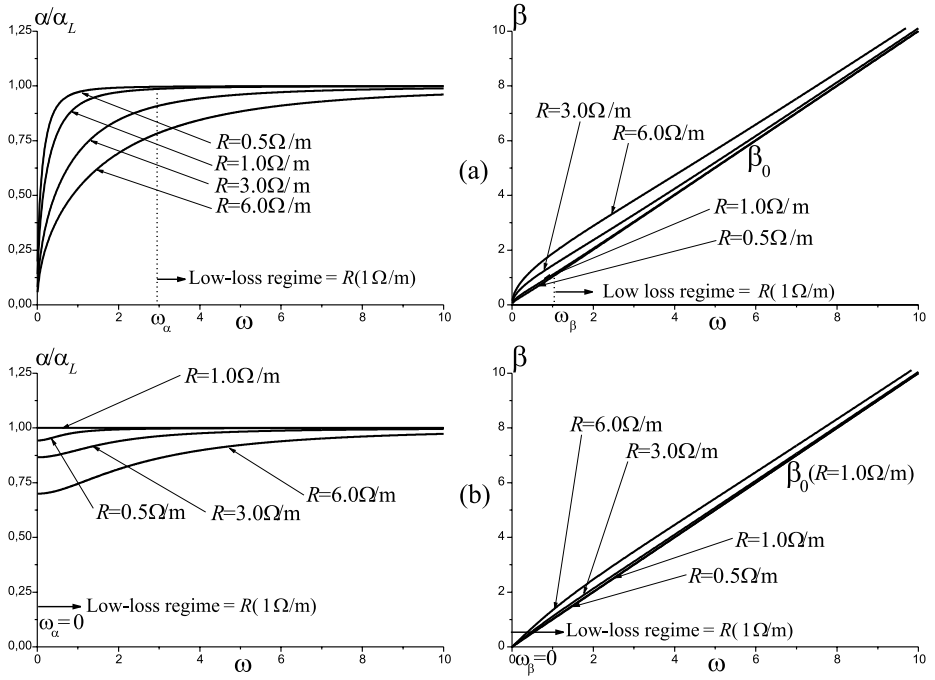

Figure 6. Representation of the propagation constant, $\gamma = \alpha + j\beta$, in terms of R when $L = 1$ H/m, and $C = 1$ F/m, for the cases with: (a) $G = 0$ $(\Omega\mathrm{m})^{-1}$, and $G = 1$ $(\Omega\mathrm{m})^{-1}$. The corresponding low-loss regimes (ω_α and ω_β), approximated in (a) and exact in (b), are indicated for the case with $R = 1$ Ω/m.

these magnitudes through its imaginary part β. It is easy to prove that equation (6), defined in terms of $\gamma(\omega) = |\gamma|\, e^{j\varphi_\gamma}$, verifies the following condition in function of the behavior of Z_s and Y_p,

$$|\gamma| > 0, \qquad \varphi_\gamma \in (0, \pi/2]. \tag{20}$$

The valid geometrical locations of the propagation constant in the γ-complex plane will be as shown in Figure 4(b). Denoting by $\beta_0 = \omega\sqrt{LC}$ the phase constant in a lossless transmission line, with $\gamma_0 = j\beta_0$, the attenuation and phase constants may then be written as,

$$\alpha, \beta = \frac{\beta_0}{\sqrt{2}} \left[\left[\left(1 + \frac{R^2}{\omega^2 L^2}\right) \left(1 + \frac{G^2}{\omega^2 C^2}\right) \right]^{1/2} \mp \left(1 - \frac{RG}{\omega^2 LC}\right) \right]^{1/2}. \tag{21}$$

Notice that $\alpha \to 0$ and $\beta \to \beta_0$ when $R \to 0$ and $G \to 0$, which correspond to the results obtained for the ideal case. Figure 6 shows the variation of α and β in (21) for the same cases analyzed in Figure 5. The value $\alpha_L = R/2Z_{c0} + GZ_{c0}/2$ corresponds to the low-loss approximation value for α as will be analyzed next.

3.3. Phase velocity of the incident and reflected waves

Once the propagation constant has been analyzed, it is easy to determine the phase velocity for a lossy transmission line by following the usual expression $c_e = \omega/\beta$, obtaining

$$c_e = \frac{\sqrt{2}}{\left[\left[\left(1 + \frac{R^2}{\omega^2 L^2}\right) \left(1 + \frac{G^2}{\omega^2 C^2}\right) \right]^{1/2} + \left(1 - \frac{RG}{\omega^2 LC}\right) \right]^{1/2}} c_{e0}, \tag{22}$$

with $c_{e0} = 1/\sqrt{LC}$ denoting the phase velocity for the lossless case when $R = G = 0$. It is easy to verify that for any values of R, L, G and C, the phase velocity in a lossy transmission line is always less or equal to that in the ideal case, $c_e \leq c_{e0}$. Figure 7 shows the phase velocity for the cases presented in Figures 5 and 6.

3.4. Loss effects

From the analyses of Z_c and γ together with equations (1) and (2), it is possible to summarize the effects due to losses as follows:

1. The effect associated to the fact that $|Z_c| \neq Z_{c0}$, which means that the relationship between the amplitude of the incident waves v^+ and i^+ (or the reflected waves v^- and i^-) is different from their relation in the lossless case.

2. The effect associated to the fact that $\varphi_{Z_c} \neq 0$, which means that the maximum/minimum of the incident waves v^+ and i^+ (or the reflected waves v^- and i^-) do not occur at the same instants in time, as it happens in the lossless case.

3. The effect associated to the fact that $\alpha \neq 0$, which means that the amplitude of the incident waves v^+ and i^+ (or the reflected waves v^- and i^-) decay exponentially as the waves travel along the line. This is the usual effect associated to losses.

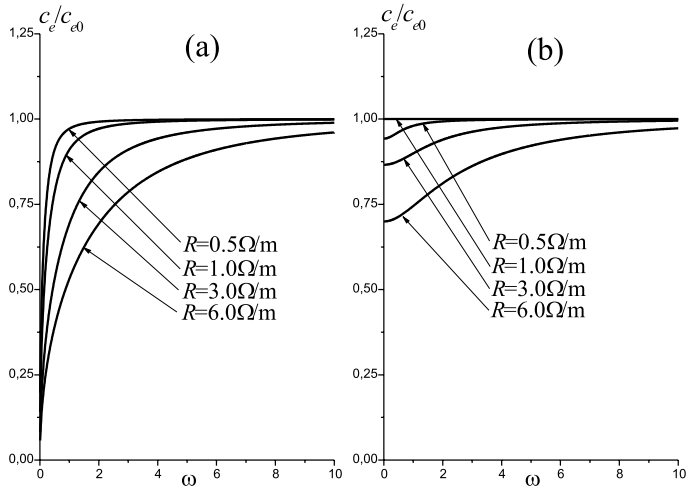

Figure 7. Phase velocity c_e in terms of R when $L = 1$ H/m, $C = 1$ F/m for: (a) $G = 0$ $(\Omega\mathrm{m})^{-1}$, and (b) $G = 1$ $(\Omega\mathrm{m})^{-1}$. The phase velocity for the lossless case is indicated with c_{e0}.

4. The effect associated to the fact that $\beta \geq \beta_0$, that is, $c_e \leq c_{e0}$ as explained in previous section.

These four effects determine the final behavior of the incident and reflected voltages and currents in a lossy transmission line, and consequently the final behavior of the total voltage and current waves observed in the lossy SWP (as that previously shown in Figure 2).

3.5. Low-loss approximation

The usual low-loss approximation, indicated with the subscript L and defined by the conditions $R << \omega L$ and $G << \omega C$, becomes now evident and better parameterized than in the usual form. From previous results, it may be noticed that there will exist a frequency f_L such that for $\omega > \omega_L = 2\pi f_L$, any basic parameter for the general lossy case approaches to certain values corresponding to those in the low-loss approximation. The value ω_L will depend on the values of R, L, G and C and will be, in general, different for any value of the basic parameters $|Z_c|$, φ_{Z_c}, α and β. Denoting by $\omega_{Z,\mathrm{mod}}$, $\omega_{Z,\mathrm{pha}}$, ω_α and ω_β the corresponding limiting values for each magnitude, it may be easily seen that,

$$\omega > \omega_{Z,\mathrm{mod}} \Rightarrow |Z_c| \rightarrow Z_{c0} = \sqrt{\frac{L}{C}}, \tag{23}$$

$$\omega > \omega_{Z,\mathrm{pha}} \Rightarrow \varphi_{Z_c} \rightarrow 0, \tag{24}$$

$$\omega > \omega_\alpha \Rightarrow \alpha \rightarrow \alpha_L = \frac{R}{2Z_{c0}} + \frac{GZ_{c0}}{2}, \tag{25}$$

$$\omega > \omega_\beta \Rightarrow \beta \rightarrow \beta_0 = \omega\sqrt{LC}. \tag{26}$$

The values in (25) and (26) may be obtained by computing the limit of (21) when $\omega L >> R$ and $\omega C >> G$. These values correspond exactly to the low-loss approximation and analytically delimit the frequency regime

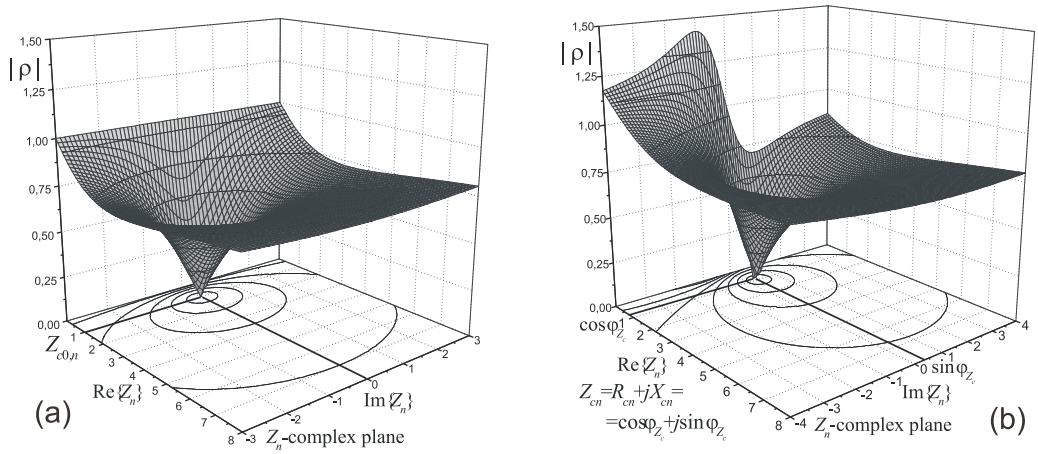

Figure 8. Amplitude of the reflection coefficient vs. $\mathrm{Re}\{Z\} > 0$ for: (a) a lossless transmission line with $Z_{c0} = \sqrt{L/C} \in \mathbb{R}$, and (b) a lossy transmission line with $\varphi_{Z_c} = 20^{\mathrm{o}}$ with the same values of L and C as in (a). In the lossless case, $Z_n = Z/Z_{c0}$; in the lossy case, $Z_n = Z/|Z_c|$ with $|Z_c| \neq Z_{c0}$.

where the approximation is valid by choosing the value ω_L as the worst case among $\omega_{Z,\mathrm{mod}}$, $\omega_{Z,\mathrm{pha}}$, ω_α and ω_β depending on the maximum relative error allowed for the approximation. These values are depicted in Figures 5 and 6 for the case with $R = 1\ \Omega/\mathrm{m}$.

Notice that there are some special cases in which the low-loss approximation is satisfied at *any frequency*. This is for the particular case in which the lossy case corresponds exactly with the low-loss case. It may be easily seen that this fact occurs when $R/L = G/C$. An example of this case is presented also in Figures 5 and 6 when $R = 1\ \Omega/\mathrm{m}$. Of course, in this special cases, the phase velocity is exactly equal to that in the lossless case, $c_e = c_{e0}$, for any frequency. Nevertheless, a word of caution is in order in those cases when the frequency range is so large that any of the line parameters (L, R, G and C) can be frequency dependent.

4. Reflection coefficient and wave impedance

4.1. Properties associated to the reflection coefficient

The general behavior of ρ in terms of Z in (9) for the lossy case is governed by the complex quantity Z_c. Notice that Z may be located within the right impedance complex semiplane, or

$$\varphi_Z \in [-\pi/2, \pi/2]. \tag{27}$$

The analysis of the absolute value of the complex mapping (9) for $\mathrm{Re}\{Z\} \geq 0$ is shown in Figure 8(b) for an example with $\varphi_{Z_c} = 20^{\mathrm{o}}$, compared with a lossless case (mantaining the values of L and C) in Figure 8(a). As may be seen, at the complex coordinate $Z = Z_c = R_c + jX_c$, $|\rho| = 0$, which is evident from (9), while the transformation has a singularity at $Z = -Z_c = -R_c - jX_c$. This value corresponds to positions of $\mathrm{Re}\{Z\} < 0$ which are excluded due to condition (27), but the function tends to increase when approaching the imaginary axis in the direction of the singularity. As it may be observed, there exist values of Z such that $|\rho| > 1$. Moreover, there is a local maximum of $|\rho|$, $|\rho|_{\max}$, which is localized at the imaginary axis $R = 0$ corresponding to the geometrical location of reactive impedances $Z = jX$. This location may be

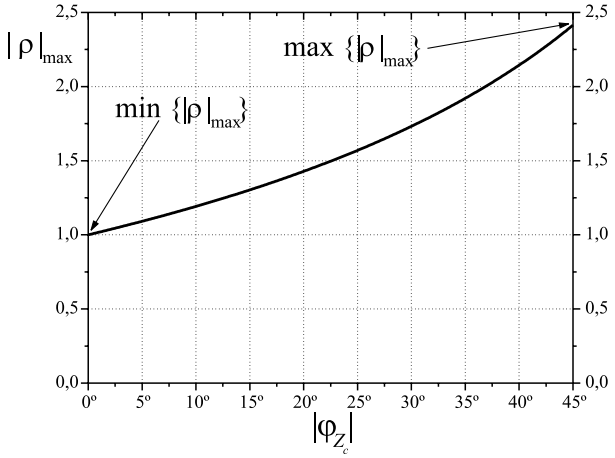

Figure 9. Typical dependence of $|\rho|_{\max}$ in terms of $|\varphi_{Z_c}|$.

easily obtained by making $R = 0$ in the expression of the absolute value of (9) and computing the first derivative with respect to X, leading to

$$|\rho|_{\max} = \sqrt{\frac{|Z_c| + |X_c|}{|Z_c| - |X_c|}}. \tag{28}$$

Once more, the general result in (28) becomes $|\rho|_{\max} = 1$ in the lossless case ($R = G = 0$) for which $|Z_c| = Z_{c0}$ real ($X_c = 0$).

4.2. Analysis of the maximum value of $|\rho|$

The main point in the analysis comes from the restriction of the possible values that Z_c may take in the complex Z-plane as seen in (17). By making $|X_c| / |Z_c| = |\sin \varphi_{Z_c}|$ in (28), $|\rho|_{\max}$ may be rewritten as,

$$|\rho|_{\max} = \sqrt{\frac{1 + |\sin \varphi_{Z_c}|}{1 - |\sin \varphi_{Z_c}|}}, \qquad \varphi_{Z_c} \in [-\pi/4, \pi/4]. \tag{29}$$

The maximum of $|\rho|_{\max}$ occurs when $|\varphi_{Z_c}| = \pi/4$ and takes the value

$$\max\{|\rho|_{\max}\} = 1 + \sqrt{2}. \tag{30}$$

It is easy to verify that the minimum value for $|\rho|_{\max}$ is

$$\min\{|\rho|_{\max}\} = 1, \tag{31}$$

and occurs when $\varphi_{Z_c} = 0$ which corresponds to the lossless case. Figure 9 shows the general representation of $|\rho|_{\max}$ in (29) versus $|\varphi_{Z_c}|$.

All these results provide a complete parameterization of the behavior of the reflection coefficient for any combination of Z and Z_c, results that will be verified later over the generalized Smith chart. A complete general analysis of the behavior of the reflection coefficient together with all the mathematical details for the lossy transmission line theory may be found in [4].

5. Generalized Smith chart

The classical Smith chart is built based on the relation between the reflection coefficient ρ and the normalized impedance $Z_n = Z/Z_{c0}$ over the (real) characteristic impedance Z_{c0} of the lossless line. The Smith chart is the representation of the real and imaginary parts of Z_n (vertical and horizontal straight lines on Z_n-plane) on the complex plane of the reflection coefficient, ρ, [5], [6]. In other words, it is a particular representation of the mapping given by eq. (10) when $Z_c = Z_{c0}$.

A generalized concept of the Smith chart for lossy transmission lines can be built analogously from (10) when $Z_c \neq Z_{c0}$ by considering a normalized impedance over the real magnitude $|Z_c|$, that is,

$$Z_n = \frac{Z}{|Z_c|}. \tag{32}$$

With this definition in mind, the complex transformation in (10) may be rewritten as

$$Z_n = R_n + jX_n = \frac{1+\rho}{1-\rho} e^{j\varphi_{Z_c}}. \tag{33}$$

Notice that both (32) and (33) reduce to the usual expressions in the lossless case ($|Z_c| = Z_{c0}$ and $\varphi_{Z_c} = 0$).

The detailed study of the complex transformation in (33) can be carried out in terms of two families of curves $R_n(\rho', \rho'')$ and $X_n(\rho', \rho'')$ which completely parameterize Z_n in the complex ρ-plane, $\rho = \rho' + j\rho''$, in a similar way as the usual Smith chart for the lossless case. The new representation may be obtained by considering the transformation

$$Z_{n1} = \frac{1+\rho}{1-\rho}, \tag{34}$$

expression which is identical to that existing between Z_n and ρ which was the basis for the classical Smith charts. The real and imaginary parts of (34) can be written as,

$$R_{n1} = \frac{1-(\rho'^2+\rho''^2)}{(1-\rho')^2+\rho''^2}, \tag{35}$$

$$X_{n1} = \frac{2\rho''}{(1-\rho')^2+\rho''^2}. \tag{36}$$

Eqs. (35)-(36) have the same representations in the complex ρ-plane as the well-known for the Smith chart.

From (33) and (34) it is possible to writte the following relationship between Z_n and Z_{n1},

$$Z_{n1} = Z_n e^{-j\varphi_{Z_c}}, \tag{37}$$

which indicates that Z_{n1} may be obtained from Z_n by performing a rotation determined by the angle $-\varphi_{Z_c}$. The complete definition of the generalized Smith chart may be understood by performing the steps summarized in the following subsections. A complete description may be found in [4].

5.1. Complex mapping from Z_n to Z_{n1}

The transformation (37) may be separated into its real and imaginary parts in the form,

$$R_{n1} = R_n \cos\varphi_{Z_c} + X_n \sin\varphi_{Z_c}, \tag{38}$$

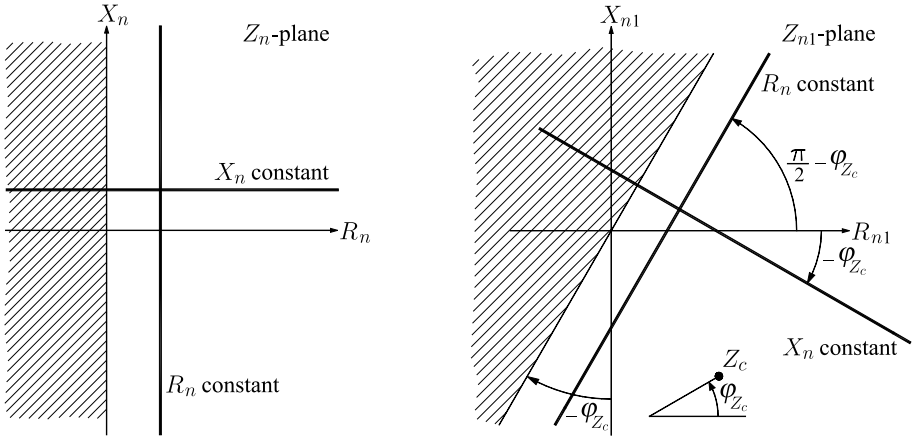

Figure 10. Transformation from the Z_n-complex plane to the Z_{n1}-complex plane.

$$X_{n1} = -R_n \sin\varphi_{Z_c} + X_n \cos\varphi_{Z_c}, \tag{39}$$

with

$$\varphi_{Z_c} \in [-\pi/4, \pi/4] \tag{40}$$

from (17). This transformation produces a rotation of an angle $-\varphi_{Z_c}$ around the origin as shown in Figure 10. Notice that the general property of $\mathrm{Re}\{Z_n\} = R_n \geq 0$ is no longer valid in the complex Z_{n1}-plane due to the rotation. Its real part may be easily obtained as

$$R_{n1} = \frac{R_n R_c + X_n X_c}{|Z_c|}, \tag{41}$$

expression which may be negative, with $R_n \geq 0$, depending on the value of X_n.

The curves which will define the generalized Smith chart are, as in the ideal case, those satisfying $R_n =$constant and $X_n =$constant. The first family of curves $Z_{n1}(R_n)$ may be obtained by eliminating X_n in (38)-(39), thus obtaining the equation

$$X_{n1} = \frac{1}{\tan\varphi_{Z_c}} R_{n1} - \frac{R_n}{\sin\varphi_{Z_c}}, \tag{42}$$

representing a straigh line for each value of R_n. The second family of curves $Z_{n1}(X_n)$ may be obtained in a similar way by eliminating R_n in (38)-(39), getting the equation namely,

$$X_{n1} = -\tan\varphi_{Z_c} R_{n1} + \frac{X_n}{\cos\varphi_{Z_c}}, \tag{43}$$

representing another straight line for each value of X_n. Next, the analysis of these line families in the complex ρ-plane will be carried out.

5.2. Family of curves with constant R_n

The family of curves $R_n =$constant in terms of ρ may be obtained by introducing the values of R_{n1} and X_{n1} given by (35) and (36) into equation (42). After some algebra, it is possible to obtain the following

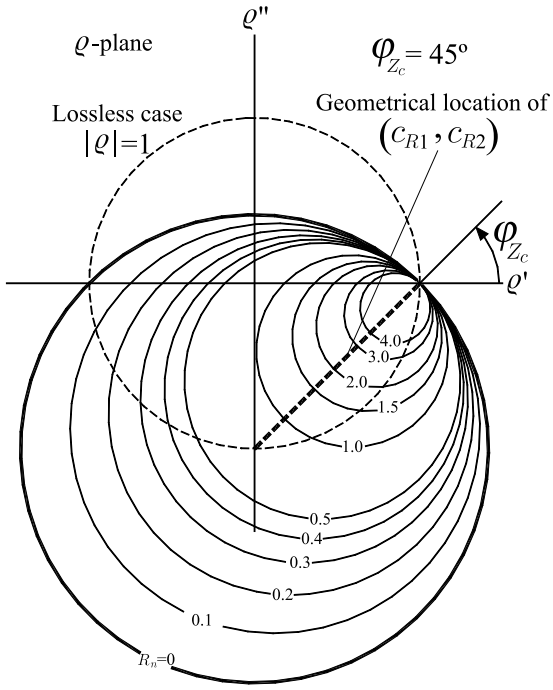

Figure 11. Family of circumferences with R_n=constant for the limiting case with $\varphi_{Z_c} = 45^o$. The circumference corresponding to $R_n = 0$ is indicated in red. The reference circumference corresponding to the lossless case is indicated in blue.

expression,

$$(\rho' - c_{R1})^2 + (\rho'' - c_{R2})^2 = r_R^2, \tag{44}$$

with

$$\begin{cases} c_{R1} = \dfrac{R_n}{R_n + \cos\varphi_{Z_c}}, \\ c_{R2} = \dfrac{-\sin\varphi_{Z_c}}{R_n + \cos\varphi_{Z_c}}, \end{cases} \tag{45}$$

and

$$r_R = \frac{1}{R_n + \cos\varphi_{Z_c}}. \tag{46}$$

Equation (44) represents a family of circumferences centered at $(\rho', \rho'') = (c_{R1}, c_{R2})$ and with radius r_R. Depending on the value of the phase of Z_c, (17), the family of circumferences is different. Figure 11 shows an example of these curves when φ_{Z_c} takes the extreme value of 45°.

5.3. Family of curves with constant X_n

The family of curves X_n =constant in terms of ρ may be obtained by introducing the values of R_{n1} and X_{n1} given by (35) and (36) into equation (43). After some algebra, it is possible to obtain the following expression,

$$(\rho' - c_{X1})^2 + (\rho'' - c_{X2})^2 = r_X^2, \tag{47}$$

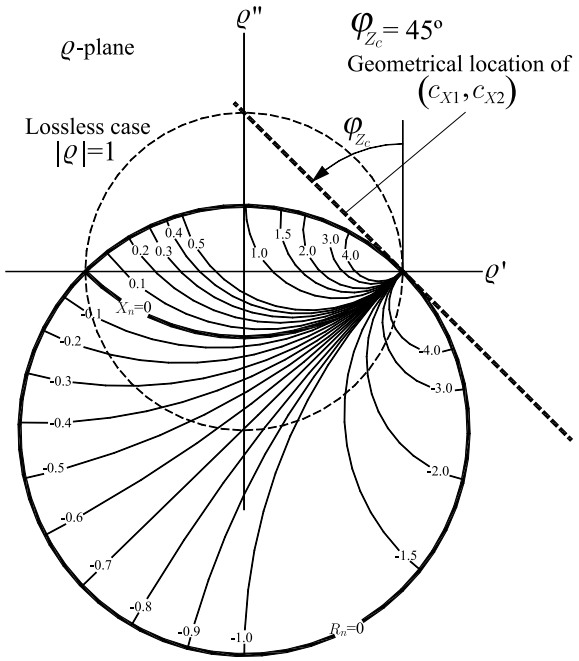

Figure 12. Family of circumferences with X_n=constant for the limiting case with $\varphi_{Z_c} = 45^o$. The geometrical location of possible values of ρ is delimited by the circumference $R_n = 0$ in red. The reference circumference corresponding to the lossless case is indicated in blue. The circunference with $X_n = 0$ is remarked in green.

with

$$\begin{cases} c_{X1} = \dfrac{X_n}{X_n + \sin\varphi_{Z_c}}, \\ c_{X2} = \dfrac{\cos\varphi_{Z_c}}{X_n + \sin\varphi_{Z_c}}, \end{cases} \tag{48}$$

and

$$r_X = \frac{1}{|X_n + \sin\varphi_{Z_c}|}. \tag{49}$$

Equation (47) represents a family of circumferences centered at $(\rho', \rho'') = (c_{X1}, c_{X2})$ and with radius r_X. Depending on the phase of Z_c, the family of circumferences will be different. Figure 12 shows an example of these curves when φ_{Z_c} takes the extreme value of 45°.

5.4. Definition of the generalized Smith chart

The joint representation of both families of circumferences in (44) and (47) for a given value φ_{Z_c}, defines the generalized Smith chart for a lossy transmission line. Its representation will depend on the phase of the characteristic impedance together with condition (17). An example of the generalized Smith chart for the limitig value $\varphi_{Z_c} = -\pi/4$ is shown in Figure 13. This picture has been generated by following a similar scheme to the usual Smith chart for the lossless case. The origin of the complex ρ-plane is indicated with $\rho = 0$ and the lossless limit $|\rho| = 1$ of the ideal Smith chart intersecting the present case is depicted with dashed line as a reference.

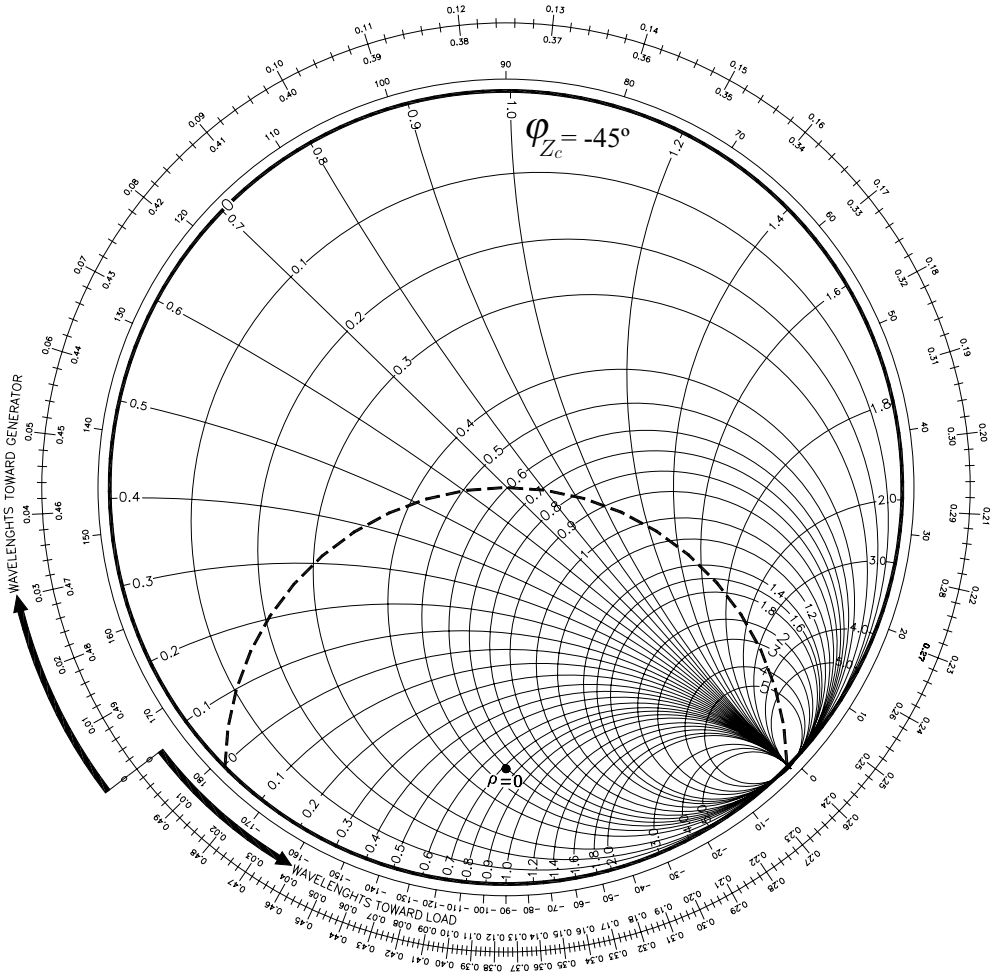

Figure 13. Example of the generalized Smith chart for the limiting value $\varphi_{Z_c} = -\pi/4$. The circumference in dashed line corresponds to the lossless case limit (Smith chart) determined by $|\rho| = 1$. The origin of the complex ρ-plane is also underlined.

Basic properties. The basic properties of the generalized Smith chart may be analyzed by studying the representation of the geometrical location of the most important impedance values on it. This study must be done by using φ_{Z_c} as main parameter. The general representation for different values of φ_{Z_c} is shown in Figure 14.

- *Ideal Smith chart.* The family of circumferences in (44) and (47) become the usual Smith chart for the ideal case when Z_c is real. This case is shown in Figure 14(d) as the intermediate case in the sequence of pictures for φ_{Z_c} varying from $-45°$ to $45°$.

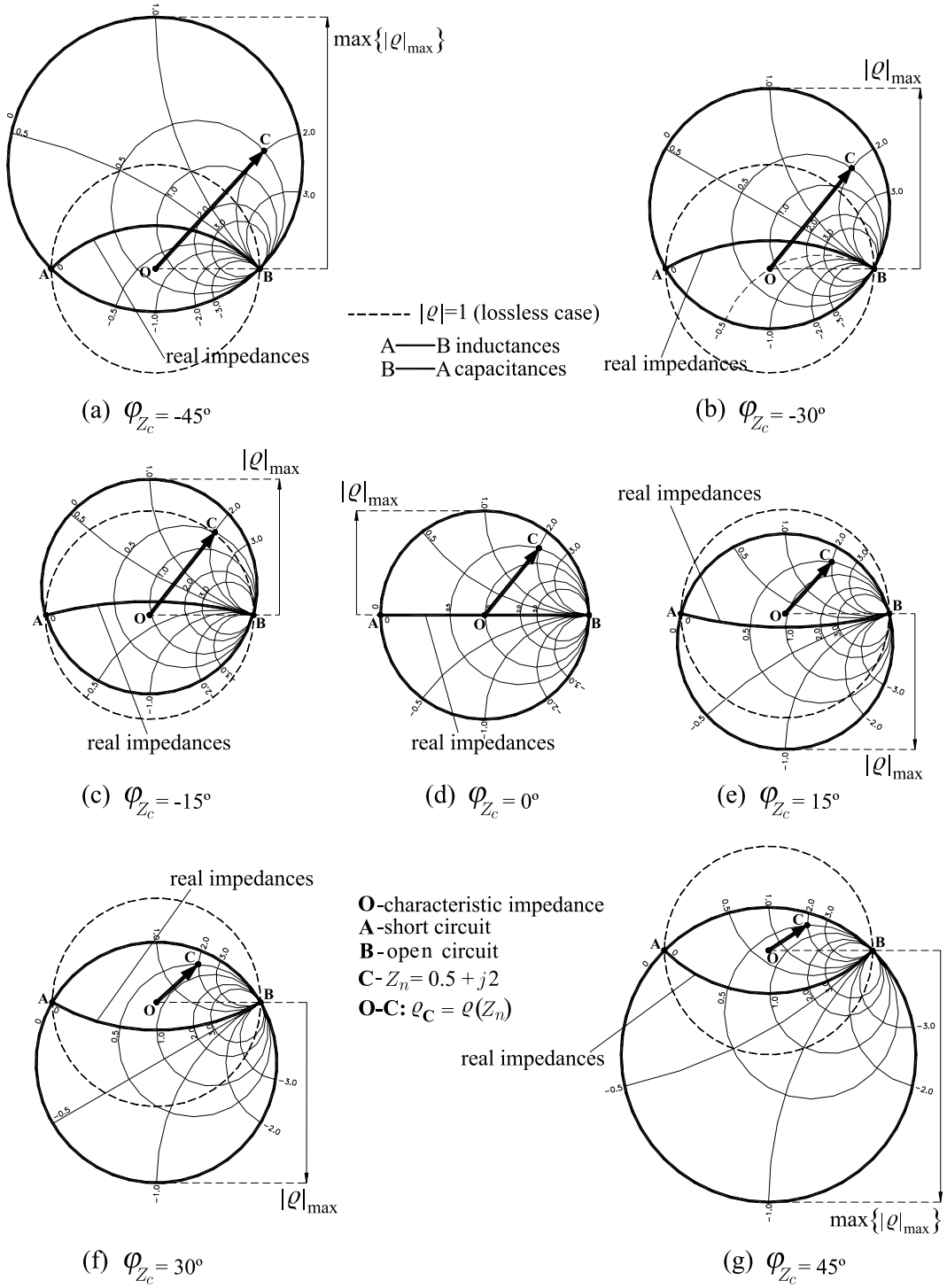

Figure 14. Schematic representation of several Smith charts for the cases with (a) $\varphi_{Z_c} = -\pi/4$, (b) $\varphi_{Z_c} = -\pi/6$, (c) $\varphi_{Z_c} = -\pi/12$, (d) $\varphi_{Z_c} = 0$, (e) $\varphi_{Z_c} = \pi/12$, (f) $\varphi_{Z_c} = \pi/6$, and (g) $\varphi_{Z_c} = \pi/4$. The case in (d) corresponds to the usual Smith chart defined for the lossless case. All the representations include: (i) an example of a normalized impedance $Z_n = Z/|Z_c| = 0.5 + 2j$, (ii) the geometrical location of resistive, inductive and capacitive impedances, and (iii) the characteristic impedance, always located at the origin of ρ-plane. All the figures include the ideal $|\rho| = 1$ circumference as a reference.

- *Reflection coefficient.* The reflection coefficient $\rho(Z)$ associated to a concrete impedance Z continues being the vector from the origin of the complex ρ-plane to the point representing the normalized impedance Z_n in the generalized Smith chart due to the general definitions in (9) and (10). Figure 14 shows an example of the different values of ρ for $Z_n = 0.5 + 2j$ as φ_{Z_c} goes from -45° to 45°.

- *Reactive impedances.* Any imaginary impedance $Z = jX$ is related to its normalized value $Z_n = jX_n = jX/|Z_c|$, which means that the geometrical location will be the circumference determined by (44)-(46) when $R_n = 0$. This curve limits the region in which all the possible values of impedances will be represented in the complex ρ-plane. For a given value φ_{Z_c}, the maximum distance from the circumference to the origin is given by $|\rho|_{\max}$ as seen in (29) and as indicated also in Figure 14. Of course, when $\varphi_{Z_c} = \pm 45^{\circ}$, the maximum distance takes its maximum value given by $\max\{|\rho|_{\max}\} = 1 + \sqrt{2}$ as obtained in (30). These values are depicted in Figures 14(a) and 14(g).

- *Resistive impedances.* Any resistive impedance $Z = R$ has a normalized value $Z_n = R_n = R/|Z_c|$. Its geometrical location will be the portion of circumference $X_n = 0$ located within the limiting curve $R_n = 0$. Any resistance will be located on this curve with its representation running from the point representing the zero impedance of a short circuit (points A in Figure 14) to the point representing the infinite impedance of an open circuit (points B in Figure 14). This curve is depicted in Figure 14 for both inductive and capacitive impedances. Notice that the general circumference for $\varphi_{Z_c} \neq 0$ degenerates into the real axis $\rho'' = 0$ in the lossless case as shown in Figure 14(d).

- *Characteristic impedance.* The complex value Z_c normalized with respect to its absolute value becomes $Z_{cn} = Z_c/|Z_c| = e^{j\varphi_{Z_c}}$. This means that its general representation will be the intersection between the circumferences $R_n = \cos\varphi_{Z_c}$ and $X_n = \sin\varphi_{Z_c}$. This intersection always reduces to the origin $\rho = 0$, which gives a constant geometrical location in the complex ρ-plane.

More details about the generalized Smith chart as well as particular analysis of practical examples using this chart may be found in [4].

6. Some examples

A first example of a simple analysis in the generalized Smith chart may be inferred directly from the basic properties presented in Sec. 5.4. Notice that Figure 14 shows the variation of the reflection coefficient ρ for a given impedance (in the example, $Z_n = Z/|Z_c| = 0.5 + 2j$) in terms of the phase of the characteristic impedance. As φ_{Z_c} depends on the loss parameters R and G, (19), Figure 14 is showing in fact an example of which is the variation of the reflection coefficient for a fixed load in terms of losses.

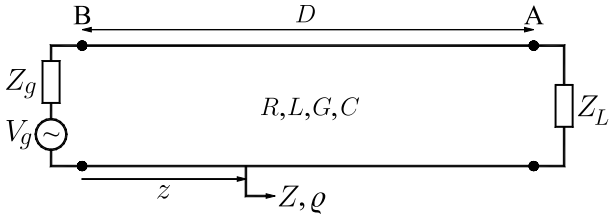

Figure 15. Transmission line circuit for the examples in Figures 16-19.

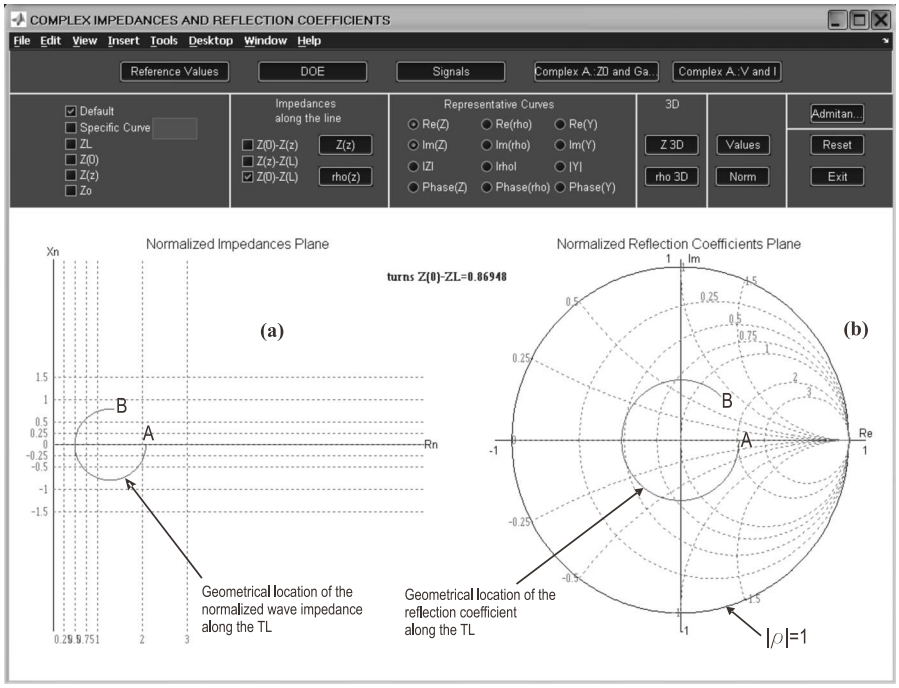

Figure 16. Lossy transmission line circuit for the example in Table. The analysis is performed on the usual Smith chart ($\varphi_{Z_c} = 0^{\circ}$). The graph in (a) shows the corresponding analysis in the complex Z_n-plane, with $Z_n = Z/Z_{c0}$, $Z_{c0} = 4.83\ \Omega$.

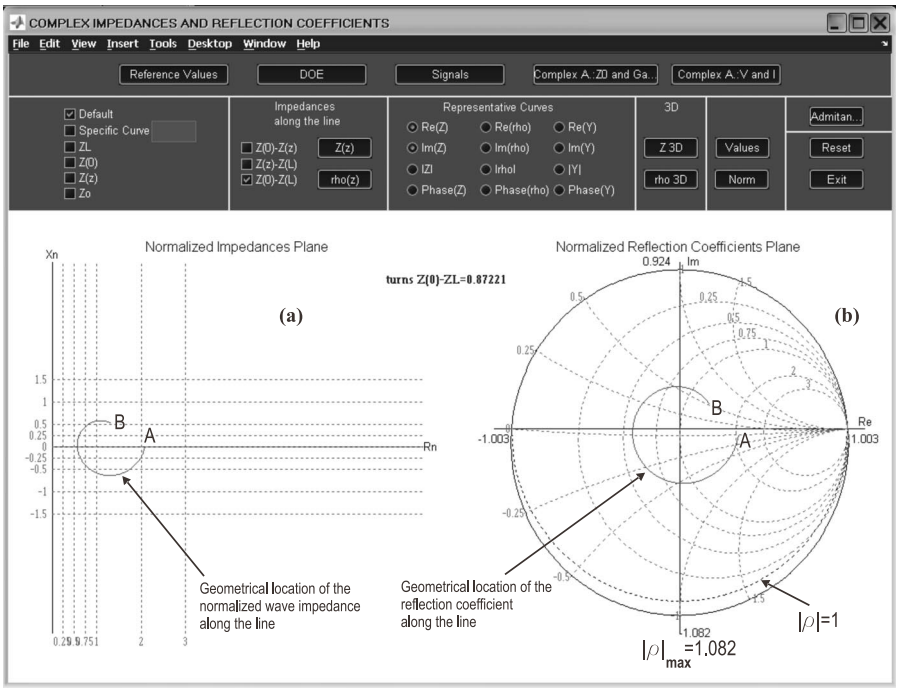

Figure 17. Lossy transmission line circuit for the example in Table. The analysis is performed in the generalized Smith chart with $\varphi_{Z_c} = 4.522^{\circ}$. The graph in (a) shows the corresponding analysis in the complex Z_n-plane, with $Z_n = Z/|Z_c|$, $|Z_c| = 4.785\ \Omega$.

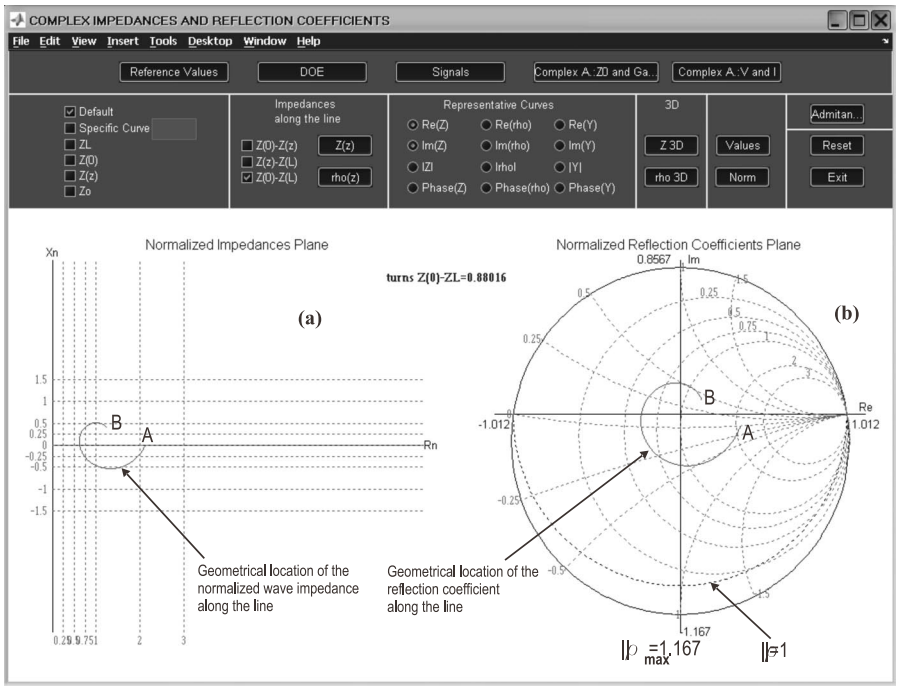

Figure 18. Lossy transmission line circuit for the data given in Table 1(c). The analysis is performed in the generalized Smith chart with $\varphi_{Z_c} = 8.828^{o}$. The graph on the left side shows the corresponding analysis in the complex Z_n-plane, with $Z_n = Z/|Z_c|$, $|Z_c| = 4.715\ \Omega$.

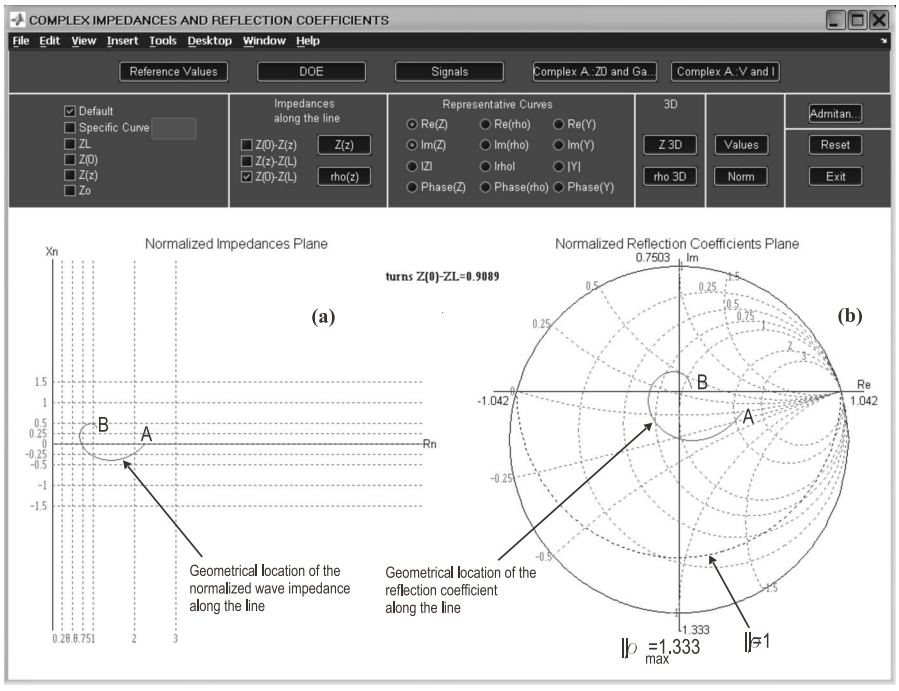

Figure 19. Lossy transmission line circuit for the data given in Table 1(d). The analysis is performed in the generalized Smith chart with $\varphi_{Z_c} = 16.24^{o}$. The graph on the left side shows the corresponding analysis in the complex Z_n-plane, with $Z_n = Z/|Z_c|$, $|Z_c| = 4.437\ \Omega$.

Table shows the data corresponding to four different examples of the analysis of a transmission line circuit as that shown in Figure 15 characterized by the following values: $f = 1$ GHz, $V_g = 1.6$ mV, $Z_g = 5$ Ω, $Z_L = 10$ Ω, $D = 0.3$ cm, $L = 0.7$ μH/m, $C = 30$ nF/m and $R = 0$ Ω/m. The analysis is based on the assumption that all these values are fixed; the only value which will vary are the dielectric losses determined by the value of G. The case in (a) corresponds to $G = 0$ $(\Omega\text{m})^{-1}$ which will be the case for the circuit with a lossless transmission line. Figure 16(b) shows the usual Smith chart and the geometrical location of $\rho(z)$ along the transmission line (from points A to B); the corresponding mapping in the complex Z_n-plane is shown in Figure 16(a). Figures 17-19 show similar analyses for different values of G, leading to $\varphi_{Z_c} = 4.522^{\text{o}}$, $\varphi_{Z_c} = 8.828^{\text{o}}$ and $\varphi_{Z_c} = 16.24^{\text{o}}$, respectively. As soon as G increases, the generalized Smith charts for the corresponding values of φ_{Z_c} must be used, leading also to different geometrical locations of $\rho(z)$ along the transmission line in the complex ρ-plane; the mappings into the Z_n-plane are also shown for the cases under analysis.

From these examples it is possible to notice that $|Z_c| \approx Z_{c0}$, $\beta \approx \beta_0$, and $\alpha \approx \alpha_L$, which corresponds to the low-loss approximation in Sec. 3.5; it is the parameter $\varphi_{Z_c} \neq 0$ who really determines the difference between the lossy and the low-loss behaviors. This results corresponds to the fact that the generalized Smith chart becomes parameterized only in terms of φ_{Z_c}.

Table

Case (a)	$Z_{c0} = 4.83$ Ω	$\varphi_{Z_c} = 0^{\text{o}}$	Figure 16
$G = 0$ $(\Omega\text{m})^{-1}$	$\alpha = 0$ m^{-1}	$\beta_0 = 910.5$ rad/m	$\lambda_0 = 0.69$ cm
Case (b)	$\lvert Z_c\rvert = 4.785$ Ω	$\varphi_{Z_c} = 4.522^{\text{o}}$	Figure 17
$G = 30$ $(\Omega\text{m})^{-1}$	$\dfrac{\alpha}{\alpha_L} = 0.9969$	$\dfrac{\beta}{\beta_0} = 1.003$	$\lambda = 0.6879$ cm
Case (c)	$\lvert Z_c\rvert = 4.715$ Ω	$\varphi_{Z_c} = 8.828^{\text{o}}$	Figure 18
$G = 60$ $(\Omega\text{m})^{-1}$	$\dfrac{\alpha}{\alpha_L} = 0.9879$	$\dfrac{\beta}{\beta_0} = 1.012$	$\lambda = 0.6817$ cm
Case (d)	$\lvert Z_c\rvert = 4.437$ Ω	$\varphi_{Z_c} = 16.24^{\text{o}}$	Figure 19
$G = 120$ $(\Omega\text{m})^{-1}$	$\dfrac{\alpha}{\alpha_L} = 0.9566$	$\dfrac{\beta}{\beta_0} = 1.045$	$\lambda = 0.6601$ cm

7. Conclusions

As it has been presented in this paper, the lossy transmission line theory constitutes a very important step when trying to analyze and understand the usual lossless case, which may be seen as a particular case of the general theory. The meaning of the usual describing parameters, that is, the characteristic impedance and the propagation constant, as well as the associated reflection coefficient and wave impedance parameters, becomes generalized, opening a major scope of their general behavior and possible values. It is also an important theory when trying to clarify and understand the low-loss regime since all the basic parameters should be studied independently in order to understand the usual approach.

On the other side, the extension of the Smith chart concept to the general lossy case provides a clean graphical visualization of the operative domain in terms of the reflection coefficient and the wave impedance for any value of the complex characteristic impedance. This particular analysis has been the basis to obtain a general complex methodology which provides a whole set of analytical parameterizations between the wave impedance, wave admittance and reflection coefficient complex planes, [4], which facilitate and extend

the understanding of all the possibilities associated to lossy transmission line problems; for instance, the analytical parameterization of the usual operations of movements on the transmission line toward load and toward generator over the generalized Smith chart, the complex wave impedance plane, and the complex wave admittance plane. These studies provide a better comprehension of the parameters which determine the solutions to a specific problem based on lossy circuits (i.e. possible values of the attenuation constant for different values of φ_{Z_c}, positions in the line where the impedances are purely real, ...) since the geometrical location of $|\rho|$ along the transmission line will lead to the typical spirals associated to the lossy case, spirals which should keep confined to the region determined by the generalized Smith chart in the complex ρ-plane, as well as their analytical transformation into Z_n- and Y_n-planes.

Finally, it is important to emphasize that all these analytical parameterizations based on complex analysis let to implement very efficient software tools which may be extensively used for educational purposes as well as designing tools in professional environments. The results shown in Figure 2, as those presented in Figures 16-19 constitute some examples of these software tools, [7].

Acknowledgments

This work has been supported by the Spanish CICYT under grant TIC2002-03121 (30 % internal founding, 70 % FEDER founding).

Note: According to the Editors' indications, the original color figures have been rendered into black and white. The originals are available upon request by mail at the following e-mail address: egr@tsc.uniovi.es.

References

[1] Cheng, D. K. *Field and Wave Electromagnetics*. Addison-Wesley Publishing Company, 1989.

[2] Pozar, D. M. *Microwave Engineering*. Addison-Wesley Publishing Company, 1990.

[3] Collin, R. E. *Foundations for Microwave Engineering*. McGraw-Hill International Editions, 1992.

[4] Emilio Gago-Ribas. *Complex Transmission Line Analysis Handbook. Vol. GW-I*. In the series Electromagnetics & Signal Theory Notebooks. GR Editores, León, Spain, June, 2001. ISBN 84-607.2514-6. (www.greditores.com)

[5] Smith, P. H. *Transmission-Line Calculator*. Electronics, vol.12, p. 29, January 1939.

[6] Smith, P. H. *An Improved Transmission-Line Calculator*. Electronics, vol. 17, p. 130, January 1944.

[7] Emilio Gago-Ribas, María J. González Morales, Carolina García Vázquez, A. Pecharroman Hernández, S. Pérez Baraja, J. C. Fernández Pérez, M. C. González Rodríguez. *Software Tool for Transmission Line Analysis*. Frontiers in Education (FIE 2000). University of Kansas. Kansas. USA. pp. S1E-10-S1E16 (Ref. 1213-CD). October, 2000.